Hindawi
Structural Control and Health Monitoring
Volume 2023, Article ID 5751636, 15 pages
https://doi.org/10.1155/2023/5751636

*Research Article*

# Cost-Effective Maintenance Policy for Sliding Surfaces of Bridge Bearings Using a Gamma Stochastic Process for Forecasting

**Xiang Xu**,[1,2] **Michael C. Forde**,[2] **Antonio Caballero**,[3] **Yuan Ren**,[1] **and Qiao Huang**[1]

[1]*School of Transportation, Southeast University, Nanjing 210096, China*
[2]*School of Engineering, University of Edinburgh, Edinburgh EH89YL, UK*
[3]*Engineering Department, Screening Eagle Technologies, Schwerzenbach 8603, Switzerland*

Correspondence should be addressed to Yuan Ren; magren@126.com

Received 28 September 2022; Revised 20 December 2022; Accepted 9 January 2023; Published 8 February 2023

Academic Editor: Suparno Mukhopadhyay



To determine the optimal alert threshold for sliding surface replacement of bridge bearings, a cost-effective maintenance policy is proposed in this paper using a gamma stochastic process. First, the sliding surface-triggered run-to-failure process of bridge bearings is discussed based on existing field inspection and maintenance records. Then, the wear thickness of sliding materials is estimated step-by-step based on the cumulative travel distance and wear rate. The gamma stochastic process is used to model degradation of sliding surfaces by using the indicator of wear thickness to depict uncertainties during the degrading process. Next, the optimal alert threshold for replacement of sliding surfaces is determined based on the cost-effective maintenance policy by minimizing the long-term expected maintenance cost rate. Finally, bearings of a long-span suspension bridge are employed to demonstrate the potential effectiveness of the proposed methodology. As a result, the wear thickness of sliding materials approximately follows a linear degrading law. Based on the gamma degrading model, the objective function subject to the long-term expected cost rate is formed. After optimization, the optimal alert threshold for replacement of sliding surfaces is 2.016 mm to achieve a minimum long-term expected maintenance cost rate of US$9,427 per day. In addition, the estimated service life subject to the alert threshold obeys a Gaussian distribution with a mean of 1278 days based on the one-year monitored displacement data.

## 1. Introduction

Bearings are critical articulation components of bridge structures, supporting the superstructure while accommodating rotational or translational movements [1, 2]. Bridge bearings not only carry static loads induced by permanent weights of superstructures but also variable forces due to traffic, temperatures, winds, and earthquakes. However, owing to the motion of bearings, they are more vulnerable, especially sliding surfaces, when compared to other components. According to existing field engineering records, the service life of sliding surfaces is frequently much lower than expected. Premature failures of sliding surfaces have been increasingly observed in recent years, especially on large-span bridges, due to unexpectedly large amounts of accumulated travel distance of girder ends, significantly weakening the serviceability of bridges [3, 4]. The failure of sliding surfaces will lead to serious defects in a short time such as locking up of bearings. The failure of bearings will result in potential damage to surrounding structural components due to increased transferred forces. For instance, the Birmingham Bridge in Pennsylvania suffered damage induced by the failure of bearings in 2008, which cost an estimated repair fee of $8 million [5]. Furthermore, the failure of bearings will change the dynamic behaviour of bridges since bearings are critical constraints for bridge structures.

Given that the traditional visual inspection is incapable of offering a timely alert on potential deterioration or malfunctioning of bearings, the long-term monitoring technology is developed to monitor the wear condition of sliding surfaces [6]. The travel distance of girder ends, i.e.,

cumulative displacement, is one of the dominant factors contributing to the wear of sliding surfaces. Displacements are mainly caused by temperatures, winds, traffic, and earthquakes, where the linear relationship between displacements and temperatures is well studied [7–10]. The temperature-induced displacement is used to estimate the maximum displacement at the bridge design stage to help choose an appropriate type of bearings or expansion joints. However, vehicle-induced dynamic displacements, rather than static ones due to temperatures, contribute to the major part of cumulative sliding displacements, which dominate the wear condition of sliding materials [4, 6, 11, 12]. Although some methodologies were proposed to estimate cumulative travel distances based on dynamically monitored data or random traffic flows [4, 13], the displacement transducer is still the most straightforward way to obtain cumulative travel distances. Newly built large-span bridges are always equipped with displacement transducers to monitor the displacement behaviour of girder ends.

In addition to cumulative travel distances, the wear rate (i.e., wear thickness per sliding distance unit) is the other key factor contributing to the wear condition of sliding surfaces. Many studies have been undertaken to investigate the tribological behaviours (i.e., friction and wear) of sliding materials (e.g., PTFE and its composites) [14–16]. Various factors, including contact pressure, temperature, lubrication, sliding surface material, sliding speed, and mating surface, influence the wear rate of sliding materials [17]. Although fruitful experiments were conducted in the lab, the size of the studied samples was relatively small compared to that of the sliding surfaces used in bridge bearings. In this regard, the size effect is the main limitation when using laboratory conclusions in tribology. Full-size experiments were designed and completed by Ala et al. [18] and Stanton et al. [19] for plain PTFE and its composites to investigate their wear behaviour. They found that the wear rate significantly depended on the contact pressure and travel speed. A model was established to determine the wear rate based on the product of contact pressure and travel speed. A relatively reliable wear rate could be estimated based on these full-size experiment results.

Based on the measured displacements and the wear rate of sliding materials, the derived wear thickness is regarded as the indicator to depict the state of sliding surfaces for condition-based maintenance [4, 11]. Although wear thickness is available continuously, an optimal alert threshold subject to maintenance operations requires further work. Existing alert/serviceability thresholds for maintenance are based on engineering experience (Table 1).

The objective of the maintenance policy could be divided into economy/availability and safety ones. For damage that has a large probability of causing tragic casualties, a safety objective is prioritized. For damage with a small probability of leading to casualties, an economy/availability objective is applied. In this paper, the topic is bearing failure triggered by the wear of sliding surfaces, which is a long-term effect under normal operational conditions. In addition, the sliding surface-triggered failure of bearings has a very low probability of causing casualties like earthquake or typhoon. Within this context, we set the economy/availability as the objective of the maintenance policy. In practice, one cannot wait until the failure level to schedule maintenance due to the large number of temporary works that may be involved. Thus, an alert threshold should be more conservative than the failure level. The optimal alert threshold is determined by maximizing the availability of the bridge or minimizing the lifetime expected cost rate. If the alert threshold is defined at a high level of wear, the probability of breakdown is large, leading to a significant cost of correction or even impacting structural or operational safety. If the alert threshold is defined at a low level of wear, the material is underutilized, resulting in higher lifetime cost.

Many stochastic maintenance models were proposed under the context of continuously monitored deteriorating systems to determine the optimal alert threshold [22, 23]. The maintenance model is first determined based on the given case, including perfect maintenance and imperfect maintenance. A perfect maintenance action restores the device to a "good or new" state [24]. For sliding surfaces of bridge bearings, the only option for maintenance actions is replacement, belonging to perfect maintenance. In addition, the stochastic model should be chosen to capture the uncertainty of the degrading process. The commonly used models contain the gamma process, Wiener process, and inverse Gaussian process. The gamma process is good at describing monotonic degradation paths, such as the degradation in the form of cumulative damage [25]. The Wiener process is more suitable for modelling degradation with nonmonotonic deterioration over time [26]. The inverse Gaussian process is a limiting compound Poisson process that is appropriate for modelling heterogeneous degradation of systems deteriorating in a random environment [27]. In this study, the gamma process is adopted since the degrading process of sliding surfaces is monotonic. Finally, the objective function is established, which aims to achieve maximum availability or the minimum cost rate. Compared to availability, bridge owners prefer to minimize the long-term expected cost rate. Therefore, a stochastic gamma process, together with perfect maintenance actions and cost-based objective functions, is desired to determine the optimal alert threshold under the context of continuous monitoring.

To determine the optimal alert threshold for replacement of sliding surfaces of bridge bearings, a cost-effective maintenance policy is proposed in this paper by assuming continuously monitored degrading systems. First, the sliding surface-triggered run-to-failure process of bearings is discussed based on existing field recorded inspection and maintenance information. Subsequently, the degrading process of sliding surfaces is developed according to the wear rate of sliding materials and monitored displacements, which is modelled by the gamma stochastic process. Next, the cost-effective maintenance model is built to consider a delayed maintenance operation, and the optimal alert threshold is proposed after optimization of the maintenance model. Finally, actual spherical bearings of a large-span suspension bridge are used to verify the effectiveness of the proposed cost-effective maintenance policy.

Table 1: Bearing replacement alert thresholds defined in codes in China, Europe, and the USA.

| Code | Alert level 1 | Alert level 2 |
|---|---|---|
| China [4, 20] | 1 mm of sliding surfaces remains: recommend replacement | 0.8 mm of sliding surfaces remains: immediate |
| Europe [21] | $h \leq 1$: more frequent inspection ($2.2\,\text{mm} \leq h \leq t_p/2.2$, where $t_p$ is the thickness of PTFE) | 0 protrusion $h$: immediate |
| USA [11] | 10%–25% of sliding surfaces remains | Na |

## 2. Methodology

Since the maintenance cost largely depends on the timing of intervention, an optimal alert threshold is developed to lower potential costs [28, 29] (see Figure 1). Monitored girder end displacement data and wear rate models of sliding materials (e.g., PTFE) are used to calculate wear thickness. Based on the wear thickness of sliding surfaces within a relatively long time window, a gamma stochastic model is used to model the thickness reduction of the sliding surface. Considering the run-to-failure process of bearings, a maintenance model is built, including maintenance plans, maintenance actions, and maintenance completions. Finally, the maintenance cost rate is set as the objective function, and the optimization algorithm is used to find the optimal thickness for replacement of the sliding surface by minimizing the cost rate.

*2.1. Sliding Surface-Triggered Run-To-Failure Process of Bearings.* There are multiple failure models for bearings in practice, such as excessive pressures and corrosion or cracking of steel components. In this paper, we focus on the sliding surface-triggered run-to-failure process.

Spherical bearings, usually used on large-span bridges, are examined. The specific configuration is demonstrated in Figure 2, which comprises upper plates, middle plates, lower plates, sliding surfaces, anchor bolts, and anchor sockets.

Although the run-to-failure process of bearings is well studied under seismic loads [30], the run-to-failure process under normal operating conditions is rarely investigated due to a lack of valid information. From inspection and maintenance records of some actual large-span bridges, the sliding surface-triggered run-to-failure process is as follows:

(1) First, with the accumulation of travel distances of girder ends, sliding materials are worn gradually, resulting in the reduction of thickness.

(2) Then, if failed sliding surfaces are not replaced timely, direct steel-to-steel contact of plates occurs, which will quickly lead to locking up of bearings.

(3) Finally, due to the requirement for motion of bridges, anchor bolts will fracture by large shear forces, leading to total failure of bearings.

The time duration from failure of sliding surfaces to total failure of bearings is quite short in practice. The total failure of bearings impacts the serviceability of bridges, leading to operational and structural safety issues. In this regard, it is assumed that the maintenance cost is equal to the potential expense of sliding surface replacement before the failure of sliding surfaces plus the potential expense of bearing replacement after the failure of sliding surfaces.

*2.2. Stochastic Degrading Model of Sliding Surfaces*

*2.2.1. Degrading Process of Sliding Surfaces.* PTFE and its composites are always adopted as the material for sliding surfaces of bridge bearings due to their high wear resistance and low friction factor. The tribological behaviour of PTFE and its composites (e.g., friction and wear) has been well studied over the past five decades [17, 31].

Various factors, including travel distance, contact pressure, temperature, lubrication, sliding surface materials, sliding speed, and mating surface, influence the wear performance and behaviour of sliding materials [19]. With the accumulation of travel distance, the wear degree of sliding surfaces increases progressively. Composite materials (e.g., glass-filled reinforced PTFE) always perform better in wear performance than the plain ones.

In general, the quantitative expression of wear volumes is

$$V_w = \int DW_v \mathrm{d}D, \tag{1}$$

where $V_w$ is the total volume reduction, $D$ is the travel distance, and $W_v$ is the wear rate in volume, namely, volume reduction per kilometer of travel distance. In practice, the wear degrees over contact areas are assumed to be uniform. Thus, Equation (1) is simplified as

$$T_w = \int DW_t \mathrm{d}D, \tag{2}$$

where $T_w$ is the total thickness reduction and $W_t$ is the wear rate in thickness, i.e., thickness reduction per kilometer of travel distance.

In equation (2), the wear rate $W_t$ is not constant and travel speed is the dominant parameter, along with pressure, temperature, lubrication, sliding surface material, and mating surface [19]. Thus, a general equation is proposed to estimate the wear rate as follows:

$$W_t = \alpha W, \tag{3}$$

where $\alpha$ is a synthetic modification factor considering the impacts of temperature, lubrication, and mating surfaces, and $W$ is a base wear rate subject to a determined sliding surface material, which is a function of the product of the travel speed $V$ and pressure $P$, termed as $W(PV)$.

Two distinct base wear rate values were observed with an increase in PV: one is associated with mild-wear regimes (low $W$) and the other is subject to severe-wear regimes (high $W$) [32]. There was an abrupt transition between the two regimes at the so-called PV limit. Figure 3 plots the measured base wear rate values with an increase in PV for plain PTFE tests performed by Ala et al. [18] and NCHRP 432 tests [19], where full-size experiments were designed and carried out. Once the value of PV exceeds the limit, the base wear rate increases quickly. Moreover, linear functions are proper to fit the measurements both in low and high wear regimes. Similar rules were found for composited PTFEs, such as ultrahigh-molecular weight PTFE and glass-filled reinforced PTFE [18]. Thus, the base wear rate is expressed as a piece-wise function to distinguish between low and high wear regimes as follows:

$$W(x) = \begin{cases} k_1 x, & x \le PV_{\text{limit}}, \\ k_2 x + b_2, & x > PV_{\text{limit},} \end{cases} \tag{4}$$

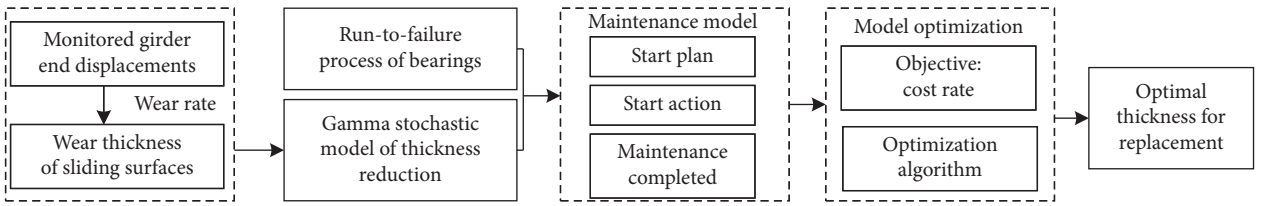


Figure 1: Flowchart of the workflow subject to the proposed cost-effective maintenance policy.

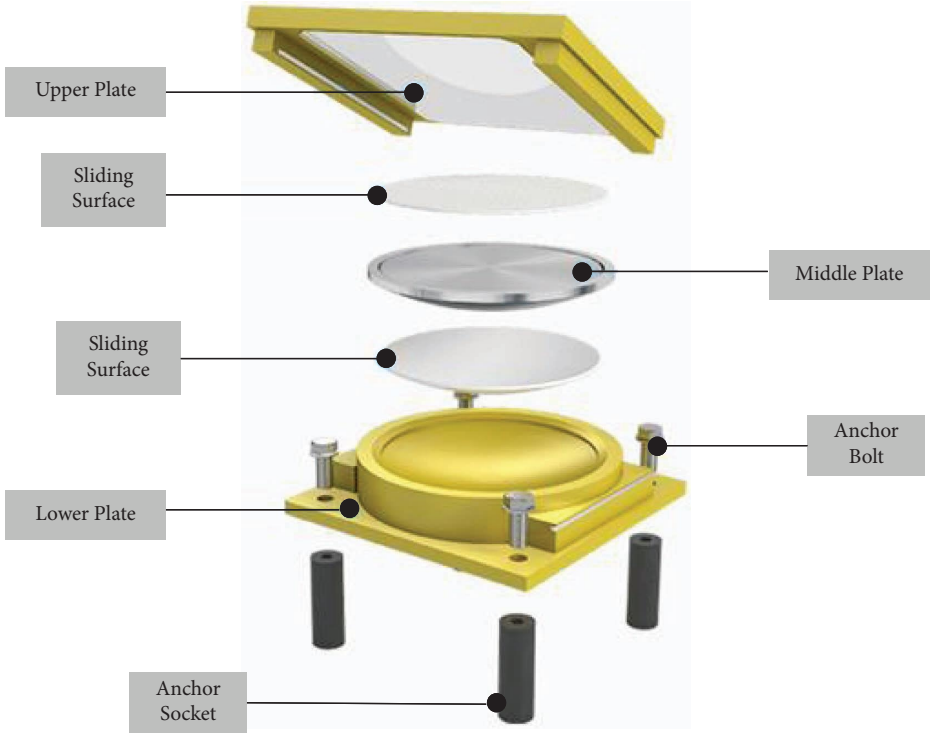


Figure 2: Configuration of spherical bearings.

where $x$ is the product of pressure and travel speed, i.e., PV, $k_1$ is the slope within the low wear regime, and $k_2$ and $b_2$ are slopes, and the $Y$-intercept corresponds to the high wear regime.

To investigate the degrading process, the degrading indicator should be defined in advance. For sliding surfaces of bearings, the wear thickness of sliding materials is regarded as a quantitative indicator to depict the wear condition of sliding surfaces. Therefore, the degrading process of sliding surfaces is defined as

$$T_w = \int \alpha D W(x) \mathrm{d}D. \tag{5}$$

The displacements of girder ends are monitored by using transducers, which could indirectly reflect wear status of sliding surfaces [33]. Thus, the monitored data of displacements should be introduced to express the degrading model of sliding surfaces. Since measurement noise largely affects calculated results, denoising is an essential data preprocessing step. Herein, the Butterworth low-pass filter with a cutoff frequency of 0.5 Hz is employed [6, 34]. According to Equation (5), the degrading process of sliding surfaces using the monitored displacement vector $(d_1, d_2, \ldots, d_N)$ is

$$T_w = \sum_{i=2}^{N} \alpha \left| d_i - d_{i-1} \right| W(x_i), \tag{6}$$

where

$$W(x_i) = \begin{cases} k_1\left(P_i f \left| d_i - d_{i-1} \right|\right), & P_i f \left| d_i - d_{i-1} \right| \le PV_{\text{limit}}, \\ k_2\left(P_i f \left| d_i - d_{i-1} \right|\right) + b_2, & P_i f \left| d_i - d_{i-1} \right| > PV_{\text{limit}}, \end{cases} \tag{7}$$

where $P_i$ is the contact pressure at instant $i$ and $f$ is the sampling frequency of displacement transducers.

The variation of pressures is not significant since the permanent load (or dead load), rather than the variable load (or live load), i.e., vehicle-induced loads, contributes to the major part of contact pressures. If the contact pressure is not monitored, the following assumption could be made. Two signature pressures are defined herein, including the permanent load/dead load pressure and all load pressure (i.e., permanent plus variable). The all load pressure is the load

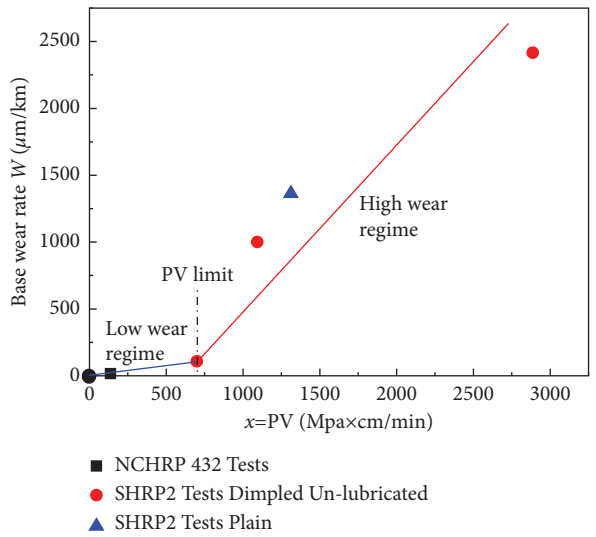


Figure 3: Variations of the base wear rate against PV for plain PTFE.

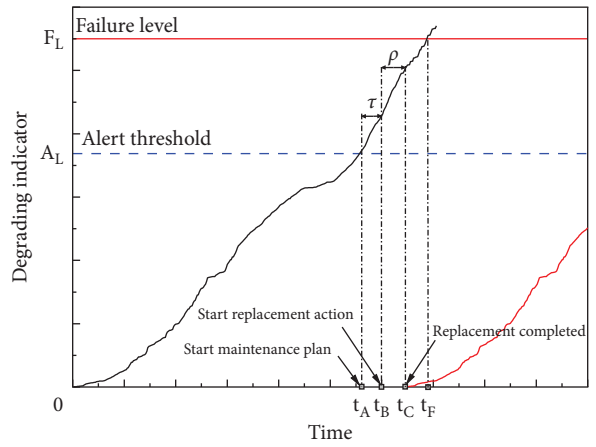


Figure 4: Description of the maintenance policy.

taken by bearings under the combined loading condition. During normal operational phases, the contact pressure will fluctuate between the permanent load and all load pressures. Thus, it is acceptable to use a normal distribution $(\mu, \sigma)$ to model the contact pressures based on permanent load and all load pressures, where

$$\mu + 3\sigma = P_D; \mu - 3\sigma = P_0, \tag{8}$$

where $P_D$ is the all load pressure and $P_0$ is the permanent load pressure.

The parameters, $k_1$, $k_2$, and $b_2$, of the linear fit are derived from existing full-scale testing results. Then, according to the product of pressure and travel speed, the base wear rate is determined, as shown in Figure 3.

The synthetic modification factor $\alpha$ should be obtained through tests. However, at present, insufficient data are available to work out the factor [11]. Until further tests are conducted, the factor is assumed to be 1 herein.

Based on the aforementioned discussions, the steps to generate the degrading process are summarized as follows:

(1) Based on the monitored displacements of girder ends, the travel distance $D_i$ from instant $(i-1)$ to $i$ is calculated as $|d_i - d_{i-1}|$.

(2) The average sliding speed $V_i$ during the time window $(i-1, i)$ is then computed as $fD_i$, where $f$ is the sampling frequency.

(3) The average contact pressure $P_i$ is randomly generated, where $P_i \sim N_P(\mu, \sigma)$.

(4) According to the product value of $P_iV_i$ and Figure 3, the base wear rate $W(P_iV_i)$ is determined.

(5) According to Equation (6), the degrading indicator $T_w$ at instant $i$ is calculated, where $\alpha$ equals to 1.

(6) We repeat steps (1)–(5), from $i = 2$ to $i = N$, where $N$ is the number of measured displacement time series.

*2.2.2. Gamma Stochastic Model.* The gamma process is a popular stochastic process to model the degrading process due to its three features: (1) independent increments, (2) not decreasing, and (3) homogeneous in time [35]. The gamma process is a Levy process that has explicit marginal probability density functions to facilitate computations. In this paper, the gamma stochastic model is applied to model the degrading process.

Replacement is the only optional maintenance action for sliding surfaces in practice. Once replacement is completed, the device is assumed to be "good or new," and the degrading indicator is set at zero. The system evolution after replacement is independent of the past. Although multiple replacement actions are conducted during the service life of bridges, the maintenance policy only needs to be studied within one replacement cycle since the degrading process of each replacement cycle is independent and identical. Within the replacement cycle of sliding surfaces, the degrading indicator $T_w(t)$ is assumed to evolve following a gamma stochastic process. The gamma process $\widehat{X}(t)$ subject to the service age $t$ has the following three attributes:

(1) $\widehat{X}(0) = 0$

(2) For all $0 \le t_i < t_j$, the increment in the degrading indicator $\widehat{X}(\delta t)$ subject to the time window $\delta t = (t_j - t_i)$ follows a gamma probability density:

$$f(x; \alpha\delta t, \beta) = \frac{\beta^{\alpha\delta t}}{\Gamma(\alpha\delta t)} x^{\alpha\delta t - 1} e^{-\beta x}, \tag{9}$$

where $\alpha\delta t$ is the shape parameter and $\beta$ is the scale parameter. The two parameters of the gamma distribution can be estimated using degrading data by the statistical procedure.

(3) $\widehat{X}(t)$ has independent increments.

### 2.3. Cost-Effective Maintenance Policy

*2.3.1. Maintenance Model.* The wear thickness of sliding surfaces is calculated continuously based on monitored displacement data. According to the continuous degrading indicator, the maintenance policy is shown in Figure 4 and specifically described as follows:

(1) When the value of the degrading indicator equals or exceeds the alert threshold $A_L$, the maintenance plan starts getting scheduled. $t_A$ denotes instant when the degrading indicator is greater than $A_L$:

$$t_A = \inf\{t: T_w(t) \ge A_L\}. \tag{10}$$

(2) When activated, a maintenance action effectively starts after a delayed duration $\tau$, i.e., at instant $t_B = t_A + \tau$. The needed delayed time before the maintenance operation is for a global maintenance setup.

(3) During the maintenance setup, failure of the whole bearing might occur. If $T_w(t_B) \le T_w(t_F)$ (where $t_F$ is the instant corresponding to the failure level $F_L$), the whole bearing functions well, and the maintenance duration is subject to the time of replacement of sliding surfaces $\rho_1$. If $T_w(t_B) > F_L$, the whole bearing fails, and the maintenance duration is the time duration of replacement of the whole bearing $\rho_2$. In this regard, the expression of the expected duration of maintenance actions is as follows:

$$E(\rho) = P(T_w(t_B) \le F_L)\rho_1 + P(T_w(t_B) > F_L)\rho_2, \tag{11}$$

where $P(T_w(t_B) \le F_L)$ is the probability that the bearing does not fail, $\rho_1$ is the time duration of replacement of sliding surfaces, $P(T_w(t_B) > F_L)$ is the probability of failure of the whole bearing, and $\rho_2$ is the time duration of replacement of the whole bearing.

(4) At the end of the maintenance operation $t_C$, the performance of sliding surfaces is as good as new, and the degrading indicator equals to zero. The degrading process of the replaced sliding surfaces is independent of the past.

Since the optimization objective of the maintenance model is to minimize the long-term expected maintenance cost rate, the cost model needs to be discussed in advance. It is noted that the degrading process shown in Figure 4 is a regenerative process with regeneration times being the dates of the end of replacement. Once replacement is completed, the degrading indicator is equal to zero, and the following stochastic evolution process is independent of the past. Therefore, the long-term expected maintenance cost rate could be regarded as the cost of the mean downtime in a cycle. The maintenance cost model consists of two parts, including the replacement cost of sliding surfaces $C_s$ and the replacement cost of the whole bearing $C_b$ based on the failure criterion. In addition, the overall cost of maintenance operations includes the economic loss due to bridge shutdowns. The specific long-term expected cost of the maintenance actions is as follows:

$$\begin{aligned} E(C) = {} & P(T_w(t_B) \le F_L)(\rho_1 C_0 + C_s) \\ & + P(T_w(t_B) > F_L)(\rho_2 C_0 + C_b), \end{aligned} \tag{12}$$

where $C_0$ is the toll loss per time unit.

*2.3.2. Model Optimization.* The objective of the proposed cost-effective maintenance policy is to minimize the long-

term expected cost per time unit by selecting a proper alert threshold value $A_L$. The objective function $U$ is set as

$$U = \frac{E(C)}{E(t_C)} = \frac{P(T_w(t_B) \le F_L)(\rho_1 C_0 + C_s) + P(T_w(t_B) > F_L)(\rho_2 C_0 + C_b)}{E(t_A + \tau + \rho)}. \tag{13}$$

Since the maintenance setup duration is constant, Equation (13) is further expressed as

$$U = \frac{P(T_w(t_B) \le F_L)(\rho_1 C_0 + C_s) + P(T_w(t_B) > F_L)(\rho_2 C_0 + C_b)}{E(t_A) + \tau + E(\rho)}. \tag{14}$$

Since the degrading process is modelled by using the gamma process, the probabilities $P(T_w(t_B) \le F_L)$ and $P(T_w(t_B) > F_L)$ can be calculated as follows:

$$P(T_w(t_B) \le F_L) = F(F_L - A_L; \alpha\tau, \beta) = \int_0^{F_L - A_L} f(x; \alpha\tau, \beta)\mathrm{d}x,$$
$$P(T_w(t_B) > F_L) = 1 - F(F_L - A_L; \alpha\tau, \beta), \tag{15}$$

where $F$ is the cumulative density function of the gamma distribution and $f$ is the probability density distribution, whose specific expression is listed in Equation (9).

To calculate $E(t_A)$, the expected wear thickness per time unit should be determined in advance, which is as follows:

$$E(T_w) = \int_0^{\infty} f(x; \alpha\tau, \beta)x\mathrm{d}x. \tag{16}$$

Then, $E(t_A)$ is derived as

$$E(t_A) = \frac{A_L}{E(T_w)} = \frac{A_L}{\int_0^{\infty} f(x; \alpha\tau, \beta)x\mathrm{d}x}. \tag{17}$$

$E(\rho)$ can be calculated by following Equation (11).

In this regard, the objective function can be expressed by the object variable $A_L$, gamma degrading process function, and known parameters (i.e., $\rho_1$, $C_0$, $C_s$, $\rho_2$, $C_b$, $\tau$, and $F_L$).

Once the objective function is obtained, the optimization algorithm is applied and summarized as follows:

(1) Estimate values of the shape and scale parameters of the gamma degrading process by using the obtained degrading data.

(2) Determine the known parameters, namely, the maintenance setup duration $\tau$, the time duration of sliding surface replacement $\rho_1$, the time duration of bearing replacement $\rho_2$, the direct expense of sliding surface replacement $C_s$, the direct expense of bearing replacement $C_b$, the expected toll loss per time unit $C_0$, and the failure level $F_L$.

(3) Start with a relatively small value of $A_L$ within the range $(0, F_L)$.

(4) Calculate the objective function listed in Equation (14) for selected $A_L$.

(5) Adjust $A_L$ by a small increment unless reaching $F_L$, and repeat steps (3) and (4).

(6) Choose the feasible value of $A_L$ to minimize the long-term expected maintenance cost rate.

*2.3.3. Service Life Prediction.* In addition, the service life corresponding to the alert threshold $A_L$ can be approximately estimated in advance of the degrading indicator reaching the alert threshold in practice. Based on the gamma degradation process, the estimated service life subject to $A_L$ is

$$N_{A_L} = \inf\left\{N: \sum_{w,i}^{N} \Delta T_{w,i} > A_L\right\}, \tag{18}$$

where $\Delta T_w$ is the degrading indicator increment in a given time step and follows the gamma distribution listed in Equation (9), namely, $\Delta T_w \sim \Gamma(\alpha\delta t, \beta)$. Since the increment $\Delta T_w$ is a stochastic variable, the estimated service life $N_{A_L}$

suffers from uncertainties. After repeating Equation (18) many times, the distribution of the service life is achieved.

The estimated service life totally depends on the gamma degrading process. The gamma process is developed based on the available degrading indicator measurements. In this regard, the estimated service life is highly related to the existing monitored data. With the accumulation of newly monitored data, the gamma process and service life will be updated accordingly.

## 3. Case Study

*3.1. The Studied Bridge.* A double-tower, single-span steel box girder suspension bridge with a 1200 m main span, a 360 m west approach viaduct, and a 480 m east approach viaduct in China is regarded as a studied object. The 40.5 m width deck accommodates four traffic lanes in each direction, and the designed traffic volume and speed limit are 100,000 vehicles per day and 100 kilometers per hour. A sophisticated structural health monitoring (SHM) system was devised and implemented for the suspension bridge to monitor environmental factors, external actions, and structural responses. The SHM system comprises various types of sensors, including strain gauges, accelerometers, global positioning system (GPS), and temperature sensors. Four displacement transducers, denoted as DSQ-DIS-T02-001, DSQ-DIS-T02-002, DSQ-DIS-T05-001, and DSQ-DIS-T05-002, were installed at the ends of girders to monitor displacements, as shown in Figure 5. The sampling frequency of the displacement transducer is 10 Hz, which satisfies the requirement to obtain high-frequency displacement components induced by vehicle loadings [4]. Since tremendous differences in cumulative travel distances between the DSQ-DIS-T02-001 and DSQ-DIS-T02-002 sensors were observed, faults of the DSQ-DIS-T02-001 and DSQ-DIS-T02-002 sensors were identified as the cause of the difference. In contrast, the measurements of the DSQ-DIS-T05-001 and DSQ-DIS-T05-002 sensors vary in a similar way, as shown in Figure 6, indicating the two transducers to be in good working order [36].

*3.2. Discussion of the Recorded Displacements.* The displacement transducer, DSQ-DIS-T05-002, was adopted for the following discussion. To study the wear condition of sliding surfaces, the cumulative travel distance is a critical factor. To understand the wear situation of sliding surfaces, the daily cumulative and total cumulative travel distances in June 2019 are calculated and plotted in Figure 7, where the Butterworth low-pass filter with a cutoff frequency of 0.5 Hz is employed for denoising. It is observed that the daily cumulative distance is relatively stable, varying between 40 m and 55 m, and the monthly cumulative distance approaches 1.5 kilometers.

In addition to the cumulative travel distance, the base wear rate is also important for the wear of sliding surfaces. According to Equation (7), the product of pressure and travel speed determines the base wear rate, where contact pressures slightly fluctuate between the permanent load pressure and all load pressure as assumed. Moreover, the travel speed can be calculated by using the monitored displacements. Time histories of travel speeds on June 1, 2019, are plotted in Figure 8, where travel speeds vary between 0 cm/s and 1.75 cm/s. The distribution of travel speeds is demonstrated in Figure 9, where the majority of the travel speeds are concentrated in the range from 0 cm/s to 0.3 cm/s.

*3.3. Site-Specific Degrading Model of Sliding Surfaces.* Prior to construction of the degrading model, variables (i.e., contact pressures and base wear rates) should be determined. According to Equation (8), the distribution of pressures is plotted in Figure 10, with the dead/permanent load contact stress $P_0 = 10.34$ MPa and all load stress PD = 17.24 MPa, according to the AASHTO code [1]. The base wear rate is generated based on Figure 3.

Based on the monitored displacements from the studied bridge in June 2019, the daily and monthly cumulative wear thicknesses of sliding surfaces are obtained and plotted in Figure 11. The daily cumulative wear thickness in June 2019 fluctuates between 0.0004 mm and 0.0015 mm, and the monthly cumulative wear thickness is approximately 0.0225 mm.

One-year data (from June 2019 to May 2020) obtained from the displacement transducer (i.e., DSQ-DIS-T05-002) are used to describe the degrading process. With the growth of travel distances, the wear thickness of PTFE, regarded as the degrading indicator, is computed, as shown in Figure 12. It is observed that the wear thickness of sliding surfaces approximately follows a linear degrading law. The estimated wear thickness in one year is 0.57 mm. Moreover, according to the visual inspection records, the reduction in the thickness of sliding surfaces was approximately 1 mm within 20 months (i.e., the annual mean is equal to 0.6 mm). The estimated annual mean thickness reduction (i.e., 0.57 mm) is in line with the inspection result (i.e., 0.6 mm), which verifies the effectiveness of the proposed degrading process.

The daily cumulative wear thickness data in one year are used to fit the gamma distribution. The histogram and gamma fit are plotted in Figure 13. The fitting results show that the shape parameter is 1.2154 subject to a time interval of one day, and the scale parameter is 0.0013.

*3.4. Cost-Effective Maintenance Policy.* The objective of the cost-effective maintenance policy is to minimize the long-term expected cost rate by selecting an optimal alert threshold. First, costs of field maintenance actions need to be investigated. It is known that the cost varies significantly for different companies. For instance, based on existing records, replacement of PTFE will cost US$111,161 and 13 weeks for a British company, while it cost US$33,585 and 6 weeks for a Chinese one in 2007 [20]. Considering the actual situation of the studied bridge, we prefer to refer to the prices in the Chinese market. Moreover, the total cost of replacement should contain two parts, which are the direct expense for replacement and the indirect cost for bridge shutdowns. Based on statistical analysis, the mean daily toll income for

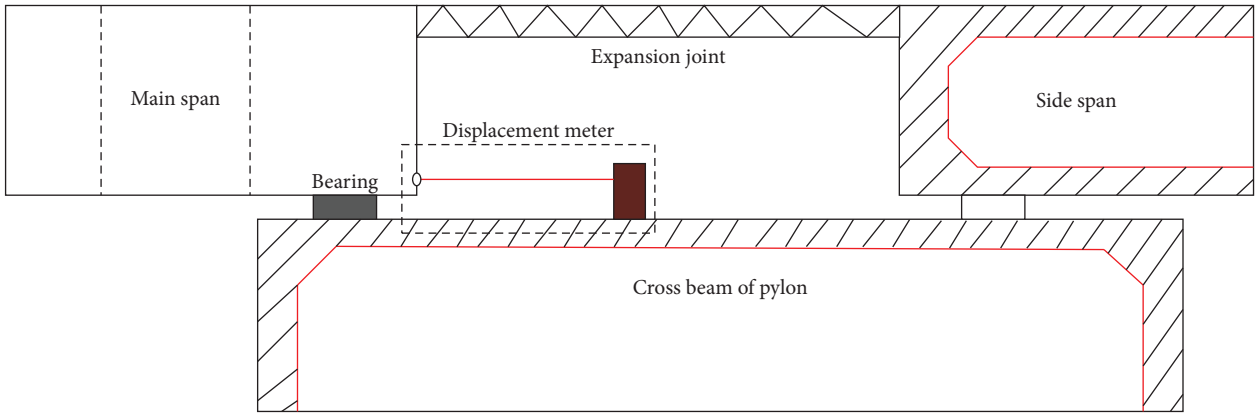


Figure 5: Layout of displacement transducers installed at the end of girders.

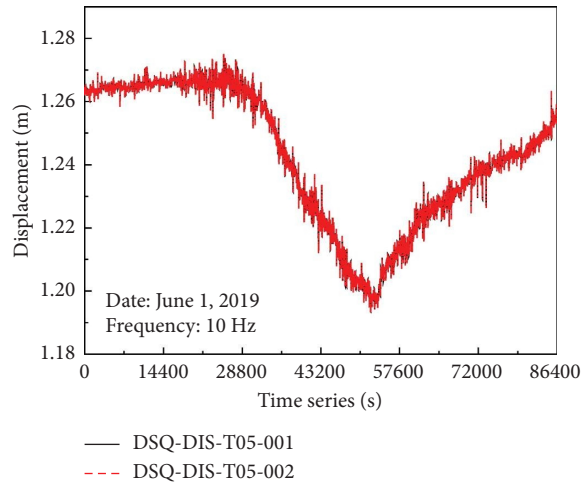


Figure 6: Displacement measurements from the two sensors on June 1, 2019.

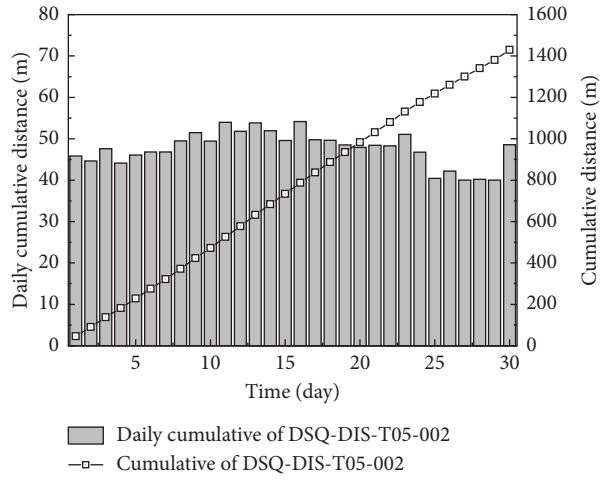


Figure 7: Daily cumulative travel distance and total cumulative travel distance in June 2019.

a similar suspension bridge is approximately US$500,000 [37]. In this paper, the influence of bridge shutdowns on the social economy is neglected since the expense is difficult to estimate within existing information.

Since no standard guideline regarding sliding surface replacement is published, the costs within the analysis are determined according to the experience and investigation. The cost subject to the replacement of sliding surfaces is

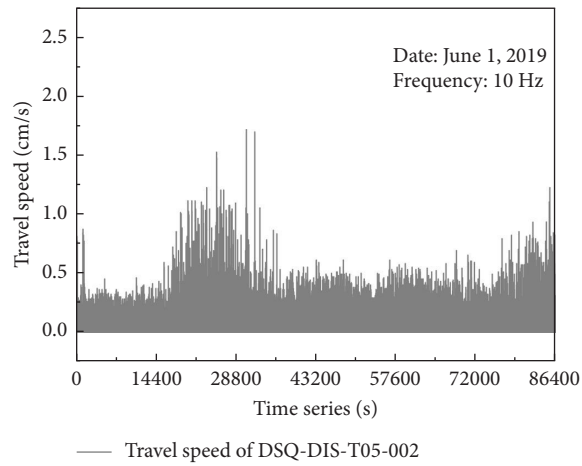


Figure 8: Travel speeds on June 1, 2019.

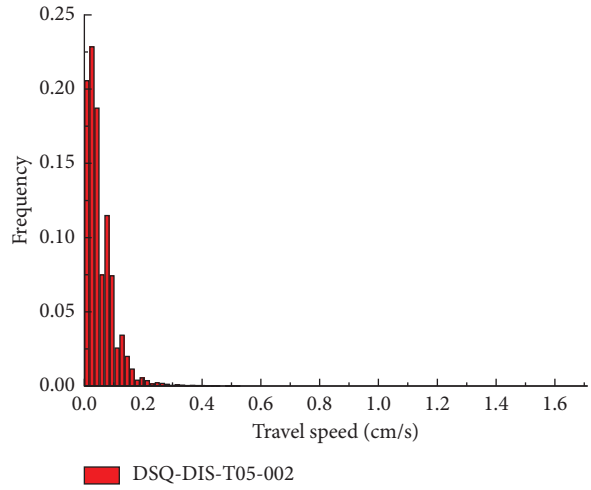


Figure 9: Statistical results of travel speeds on June 1, 2019.

estimated as US$33,585 and 6 weeks, where the mean daily loss of the toll income is US$310,980, while the cost corresponding to the replacement of bearings is US$388,726 and 12 weeks. Therefore, the total expenses for the replacement of PTFEs and bearings are US$13,094,785 and US$26,511,125, respectively. It is noticed that the major part of the expense is induced by the loss of toll income.

The maintenance setup duration is determined as three months in this case study. During the maintenance setup time, the replacement plan is first made, and then, the preparatory work follows such as material purchase and labour arrangement. The failure criterion of sliding surfaces is defined as the remaining thickness of 0.8 mm [20]. Since the initial thickness of the PTFE pad is 3 mm, the failure level is indicated by a wear thickness of 2.2 mm in this case.

The initial alert threshold $A_L$ is set at 1 mm, and the increment is determined as 0.001 mm. The long-term expected maintenance cost rate is calculated and plotted in Figure 14. With the growth of alert thresholds at an earlier stage, the long-term expected cost rate decreases since the failure probability is low and the expected service life gains. When the alert threshold approaches 2.0160 mm, the objective function reaches its lowest point. Once the alert threshold exceeds 2.0160 mm, the potential cost of failure increases to enlarge the long-term expected cost rate. Thus, the optimal alert threshold is determined as 2.0160 mm to achieve a minimum long-term expected maintenance cost rate of US$9,427 per day. The conclusion drawn from the proposed cost-effective maintenance policy is similar to that from engineering experience, which recommends replacing sliding surfaces when the wear thickness reaches 2 mm [20]. Although the conclusions are similar, this study provides a solid theoretical foundation and could be straightforwardly transferred to other case studies.

In addition, the service life of PTFE can be estimated based on the gamma degradation process. Due to the uncertainty within the degradation process, the service life subject to the alert threshold follows a Gaussian distribution with a mean of 1278 days and a standard deviation of 32 days (see Figure 15). It should be pointed out that the estimated service life totally depends on the one-year monitored

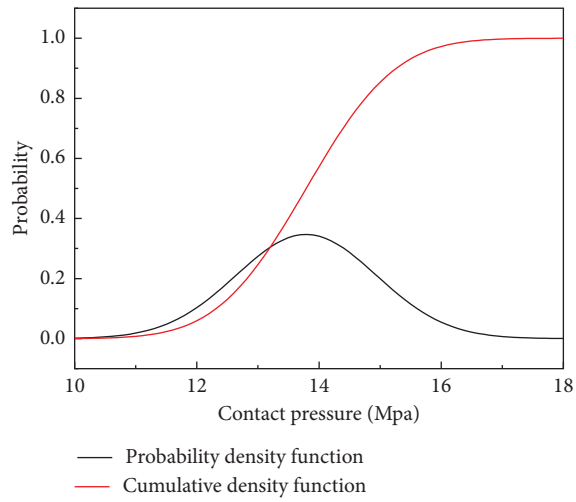


Figure 10: Distribution of contact pressures.

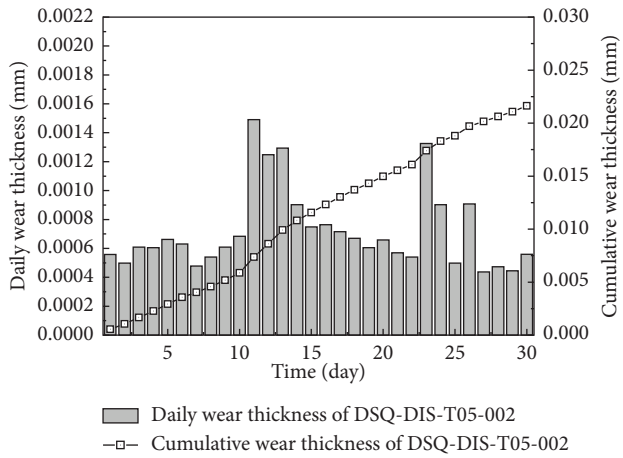


Figure 11: Daily cumulative wear thickness and total cumulative wear thickness in June 2019.

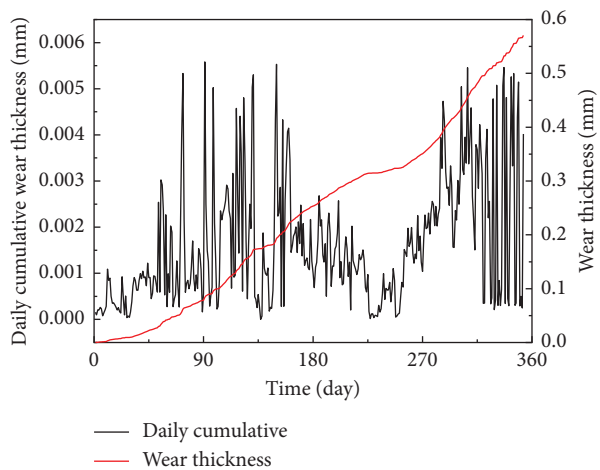


Figure 12: Daily cumulative wear thickness and total wear thickness within one year.

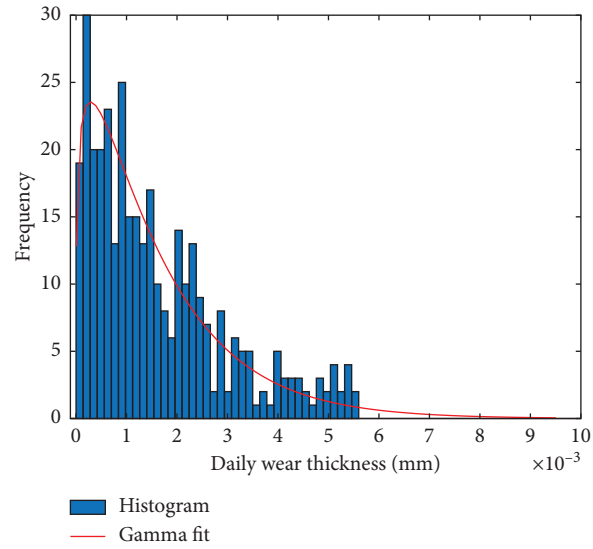


Figure 13: Histogram and gamma fit of the daily cumulative wear thickness.

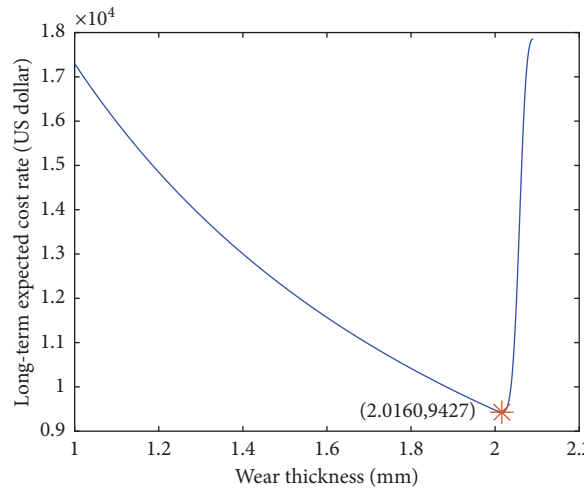


Figure 14: Long-term expected cost rate along with the potential alert threshold.

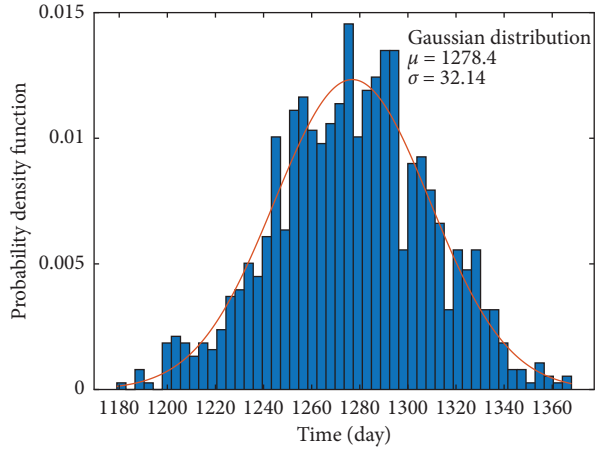


Figure 15: Distribution of the estimated service life before the alert threshold.

displacement of the girder end. With the accumulation of newly monitored data, the gamma degradation process should be updated, and the distribution of estimated service life will be updated accordingly.

## 4. Conclusions

To determine the optimal alert threshold for replacement of sliding surfaces of bridge bearings, a cost-effective maintenance policy is developed and proposed in this study to consider maintenance setup time. The following conclusions can be drawn from the research:

(1) The sliding surface-triggered run-to-failure process of bridge bearings is discussed in this study based on existing inspection and maintenance records. Three stages are observed within the failure process, including failure of sliding surfaces, locking up of bearings, and failure of entire bearings.

(2) The gamma process is used to model the degrading process of sliding surfaces by using the indicator of wear thickness, which is derived from the continuously monitored displacements and the wear rate model of sliding materials. The cumulative travel distances and sliding speeds can be derived from the measured displacements, and the base wear rate is determined by the travel speed and contact pressure. The gamma stochastic model is used to model the uncertainty within the degrading process.

(3) The optimal alert threshold is determined through optimization analysis to minimize the long-term expected maintenance cost rate, where the cost includes the direct expense of maintenance operations and the economic loss of bridge shutdowns. The objective function is built based on the potential cost of failures and service ages. The parameters in the objective function are derived from the gamma degrading model and known factors such as maintenance setup time.

(4) Bearings in the case study suspension bridge are used to validate the effectiveness of the proposed methodology. Measured displacement data of girder ends are used to build the gamma degrading model of sliding surfaces. As a result, the wear thickness of sliding materials approximately follows a linear law, and the estimated wear thickness in one year is nearly 0.57 mm based on one-year field monitored data.

(5) Based on the cost-effective maintenance model, the optimal alert threshold is determined as 2.0160 mm subject to a minimum long-term expected cost rate of US$9,427 per day. In addition, the estimated service life of PTFE before the alert threshold follows a Gaussian distribution with a mean of 1278 days and a standard deviation of 38 days.

This paper makes a contribution to decision-making of maintenance policies of sliding surfaces. In the future, full-scale experiments regarding the tribology of sliding materials are needed to calibrate the base wear rate since only limited data are available currently. Furthermore, the process from the failure of sliding surfaces to failure of the entire bearings still needs more data support for calibration. Efforts should be made to depict this process through either experimental studies or field observations.

## Data Availability

The structural health monitoring data used to support the findings of this study are available from the corresponding author upon request.

## Conflicts of Interest

The authors declare no conflicts of interest.

## Authors' Contributions

XX and YR conceptualized the study. XX was responsible for methodology, software analysis, validation, and formal analysis. XX and YR were responsible for investigation. YR and QH collected the resources. YR curated the data. XX wrote the original draft. MCF and AC wrote, reviewed, and edited the manuscript. QH supervised the study. QH and AC were responsible for project administration. MCF was responsible for funding acquisition. All the authors have read and agreed to the published version of the manuscript.

## Acknowledgments

This research was funded by the European Union's Horizon 2020 Research and Innovation Programme under Marie Skłodowska-Curie grant agreement no. 801215, the University of Edinburgh Data-Driven Innovation Programme, part of the Edinburgh and South East Scotland City Region Deal, Screening Eagle Technologies, AG, Zurich, Switzerland, and the CCCC Academician Special Project under grant nos. YSZX-03-2022-01-B and YSZX-03-2021-02-B.

## References

[1] Aashto, *AASHTO LRFD Bridge Design Specifications*, American Association of State Highway and Transportation Officials, Washington, DC, USA, 2020.

[2] X. Xu, Q. Huang, Y. Ren, X. Liu, and R. Chen, "A multisource-data-based condition assessment model for large span suspension bridges," in *Proceedings of the Transportation Research Board 96th Annual Meeting*, Washington DC, USA, August 2017.

[3] T. Guo, J. Liu, and L. Huang, "Investigation and control of excessive cumulative girder movements of long-span steel suspension bridges," *Engineering Structures*, vol. 125, pp. 217–226, 2016.

[4] G. Wu, D. Yang, T. Yi, H. Li, and H. Liu, "Sliding life prediction of sliding bearings using dynamic monitoring data of bridges," *Structural Control and Health Monitoring*, vol. 27, no. 5, Article ID e2515, 2020.

[5] B. M. Noade and T. C. Becker, "Probabilistic framework for lifetime bridge-bearing demands," *Journal of Bridge Engineering*, vol. 24, no. 7, Article ID 04019065, 2019.

[6] T. Guo, J. Liu, Y. Zhang, and S. Pan, "Displacement monitoring and analysis of expansion joints of long-span steel

bridges with viscous dampers," *Journal of Bridge Engineering*, vol. 20, no. 9, Article ID 04014099, 2015.

[7] H. B. Huang, T. H. Yi, H. N. Li, and H. Liu, "New representative temperature for performance alarming of bridge expansion joints through temperature-displacement relationship," *Journal of Bridge Engineering*, vol. 23, no. 7, Article ID 04018043, 2018.

[8] Q. Xia, Y. Xia, H. P. Wan, J. Zhang, and W. X. Ren, "Condition analysis of expansion joints of a long-span suspension bridge through metamodel-based model updating considering thermal effect," *Structural Control and Health Monitoring*, vol. 27, no. 5, Article ID e2521, 2020.

[9] Q. Xia, J. Zhang, Y. Tian, and Y. Zhang, "Experimental study of thermal effects on a long-span suspension bridge," *Journal of Bridge Engineering*, vol. 22, no. 7, Article ID 04017034, 2017.

[10] R. Kromanis, P. Kripakaran, and B. Harvey, "Long-term structural health monitoring of the Cleddau bridge: evaluation of quasistatic temperature effects on bearing movements," *Structure and Infrastructure Engineering*, vol. 12, no. 10, pp. 1342–1355, 2016.

[11] N. Ala, E. H. Power, and A. Azizinamini, "Predicting the service life of sliding surfaces in bridge bearings," *Journal of Bridge Engineering*, vol. 21, no. 2, Article ID 04015035, 2016.

[12] G. Wang, Y. Ding, H. Guo, and X. Zhao, "Safety evaluation of the wear life of high-speed railway bridge bearings by monitoring train-induced dynamic displacements," *Shock and Vibration*, vol. 2018, Article ID 6479480, 14 pages, 2018.

[13] G. Li, W. Han, X. Chen, T. Guo, Q. Xie, and Y. Yuan, "Wear evaluation on slide bearings in expansion joints based on cumulative displacement for long-span suspension bridge under monitored traffic flow," *Journal of Performance of Constructed Facilities*, vol. 34, no. 1, Article ID 04019106, 2020.

[14] Q. Yuan, G. Jun, C. Wenhan, W. Honggang, R. Junfang, and G. Gui, "Tribological behavior of PTFE composites filled with peek and nano-Al2O3," *Tribology Transactions*, vol. 61, no. 4, pp. 694–704, 2018.

[15] C. A. G. S. Valente, F. F. Boutin, L. P. C. Rocha, J. L. do Vale, and C. H. da Silva, "Effect of graphite and bronze fillers on PTFE tribological behavior: a commercial materials evaluation," *Tribology Transactions*, vol. 63, no. 2, pp. 356–370, 2020.

[16] L. Deleanu, M. Botan, and C. Georgescu, *Tribological Behavior of Polymers and Polymer Composites*no. 7–15, IntechOpen, London, UK, 2020.

[17] J. Khedkar, I. Negulescu, and E. I. Meletis, "Sliding wear behavior of PTFE composites," *Wear*, vol. 252, no. 5-6, pp. 361–369, 2002.

[18] N. Ala, E. H. Power, and A. Azizinamini, "Experimental evaluation of high-performance sliding surfaces for bridge bearings," *Journal of Bridge Engineering*, vol. 21, no. 2, Article ID 04015034, 2016.

[19] J. F. Stanton, C. W. Roeder, and T. I. Campbell, *High-load Multi-Rotational Bridge Bearings. 432*, Transportation Research Board, National Research Council, National Academies Press, Washington, DC, USA, 1999.

[20] Y. Fan and X. Chen, "Research on maintenance and replacement technology of main bridge PTFE slide bearing of the Jiangyin Yangtze River Bridge," *Modern Transportation Technology*, vol. 6, no. 6, pp. 64–66, 2009.

[21] "British standard institution. Part 2: sliding elements," *Structural Bearings*, vol. 34, 2004.

[22] X. Liu, J. Li, K. N. Al-Khalifa, A. S. Hamouda, D. W. Coit, and E. A. Elsayed, "Condition-based maintenance for continuously monitored degrading systems with multiple failure modes," *IIE Transactions*, vol. 45, no. 4, pp. 422–435, 2013.

[23] C. Chuang, L. Ningyun, J. Bin, and X. Yin, "Condition-based maintenance optimization for continuously monitored degrading systems under imperfect maintenance actions," *Journal of Systems Engineering and Electronics*, vol. 31, no. 4, pp. 841–851, 2020.

[24] B. de Jonge and P. A. Scarf, "A review on maintenance optimization," *European Journal of Operational Research*, vol. 285, no. 3, pp. 805–824, 2020.

[25] S. Alaswad and Y. Xiang, "A review on condition-based maintenance optimization models for stochastically deteriorating system," *Reliability Engineering & System Safety*, vol. 157, pp. 54–63, 2017.

[26] C. Guo, W. Wang, B. Guo, and X. Si, "A maintenance optimization model for mission-oriented systems based on Wiener degradation," *Reliability Engineering & System Safety*, vol. 111, pp. 183–194, 2013.

[27] Z. S. Ye and N. Chen, "The inverse Gaussian process as a degradation model," *Technometrics*, vol. 56, no. 3, pp. 302–311, 2014.

[28] O. Gölbaşı and N. Demirel, "A cost-effective simulation algorithm for inspection interval optimization: an application to mining equipment," *Computers & Industrial Engineering*, vol. 113, pp. 525–540, 2017.

[29] G. Levitin, L. Xing, and H. Z. Huang, "Cost effective scheduling of imperfect inspections in systems with hidden failures and rescue possibility," *Applied Mathematical Modelling*, vol. 68, pp. 662–674, 2019.

[30] H. A. Gibe, H. Tamai, and Y. Sonoda, "Numerical study on failure process and ultimate state of steel bearing under combined load," *Heliyon*, vol. 6, no. 4, Article ID e03764, 2020.

[31] K. L. Campbell, M. A. Sidebottom, C. C. Atkinson et al., "Ultralow wear PTFE-based polymer composites—the role of water and tribochemistry," *Macromolecules*, vol. 52, no. 14, pp. 5268–5277, 2019.

[32] T. I. Campbell and W. Kong, "PTFE sliding surfaces in bridge bearings," Ministry of Transportation and Communications, Research and Development, Downsview, ON, Canada, 1987.

[33] Y. Ni, Y. Wang, and C. Zhang, "A Bayesian approach for condition assessment and damage alarm of bridge expansion joints using long-term structural health monitoring data," *Engineering Structures*, vol. 212, Article ID 110520, 2020.

[34] Y. Ren, Q. Ye, X. Xu et al., "An anomaly pattern detection for bridge structural response considering time-varying temperature coefficients," *Structures*, vol. 46, pp. 285–298, 2022.

[35] N. Gorjian, L. Ma, M. Mittinty, P. Yarlagadda, and Y. Sun, *A Review on Degradation Models in Reliability Analysis*, pp. 369–384, Springer, Berlin, Germany, 2010.

[36] X. Xu, Q. Huang, Y. Ren, D. Zhao, and J. Yang, "Sensor fault diagnosis for bridge monitoring system using similarity of symmetric responses," *Smart Structures and Systems*, vol. 23, no. 3, pp. 279–293, 2019.

[37] Y. Ren, X. Xu, Q. Huang, D. Y. Zhao, and J. Yang, "Long-term condition evaluation for stay cable systems using dead load–induced cable forces," *Advances in Structural Engineering*, vol. 22, no. 7, pp. 1644–1656, 2019.